Heat transport by material-dependent heating during absorption of radiation in the water absorbed dose calorimeter

A. Krauss[*], M. Roos

Physikalisch-Technische Bundesanstalt (PTB), Fachlabor 6.23, Bundesallee 100, D-38116 Braunschweig, Germany

Abstract

Water absorbed dose calorimeters have been developed for the application as PTB standards for the dosimetry in radiation therapy with photon and electron radiation. Different detector types for various applications are available. In this paper, heat conduction effects of ''sealed'' detectors are investigated, caused by the material-dependent temperature rise during the absorption of ^{60}Co-γ-radiation in the detector walls and in the temperature probes embedded in water. The corresponding corrections can be minimized by a proper design, allowing the resulting relative standard uncertainty to be kept well below 0.1%. © 1999 Elsevier Science B.V. All rights reserved.

Keywords: Heat conduction; Finite element method; Detector cylinder; Water absorbed dose calorimeter; Therapy dosimetry

1. Introduction

Water absorbed dose is the measurand in the dosimetry for radiation therapy. A high accuracy of measurement in the determination of this quantity is achievable with the water absorbed dose calorimeter [1,2]. If it is ensured that the radiant energy imparted to water is totally converted into heat [3,4], the absorbed dose at the point of measurement is in principle simply given by the product of the specific heat capacity of water and the temperature rise at this point. The temperature rise measured is usually influenced by heat transport processes inside the calorimeter [5]. These processes must be well defined and determination of such processes must be possible.

Thus they can either be kept negligibly small by constructional measures or corrected.

Water absorbed dose calorimeters with different detectors for various applications have been developed at PTB [4–9]. In the case of the sealed detectors [9–12] considered here, the temperature sensors (thermistors) are arranged at the tip of two thin glass pipettes mounted opposite each other, along the axis, inside cylinders filled with water (Fig. 1). The whole detector is fitted into the water phantom (30 cm × 30 cm × 30 cm) by means of a PMMA (polymethylmethacrylate) mount. Since the values of the specific heat capacities and, to a lesser degree, also the values of the radiation interaction coefficients of these ''non-water'' materials deviate from those of water, absorption of the radiation (here: ^{60}Co-γ-radiation) leads to a material-dependent temperature rise of the components. For example, the cylinder wall and the glass pipettes are heated much more strongly than the

*Corresponding author. Fax: +49-0531-5926405

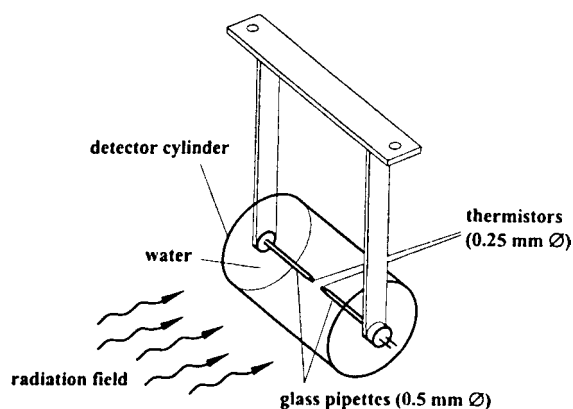*E-mail address:* achim.krauss@ptb.de (A. Krauss)

Fig. 1. The sealed detector of the water absorbed dose calorimeter (schematic view).

surrounding water, and this affects the measurement results as heat conduction takes place [10,12,13]. The strongest effect stems from the heating of the cylinder wall and depends above all on the wall thickness, the cylinder diameter and the irradiation time. Similar effects result from the irradiation of the water phantom's PMMA walls, which cannot be avoided.

In the present paper, heat transport effects caused by the material-dependent temperature rise in the detector walls and in the temperature probes embedded in water have been experimentally investigated and compared with the results of finite element calculations for different cylinder wall materials, diameters and wall thicknesses.

When these components are exposed to radiation not only the thermal effects with the respective properties enter into the results but also the radiation interactions with the respective properties, causing the heating. In order to separate some of these effects and to check the validity of the values of a few thermal parameters, the electrical heating of the thermistors has, in addition, been studied experimentally and by model calculations.

2. Materials and methods

The geometry of the water absorbed dose calorimeter and of the temperature probes was modelled with the aid of a finite element program (ANSYS 5.3) to study the effect of heat conduction for different materials, geometries and irradiation conditions.

Due to the proportions and dimensions of the calorimeter components, some investigations could be examined on the basis of two-dimensional models. The length of the detector cylinder, for example, was chosen such that in the case of a typical maximum irradiation time of 120 s the materials of the end faces did not influence the measurement results. For the computation of the influence exerted by selective heating of the glass pipettes and by the integrated thermistors, the rotational symmetry could be made use of to simplify the computations. The finite element models were built of four-node plane elements of varying geometric sizes, resulting in a total number of nodes of typically more than 10,000.

The accuracy of the computations was verified by benchmark experiments. Cylinders of different diameter and wall thickness made of glass and PMMA were used to investigate the influence of the vessel wall during irradiation with ^{60}Co-γ-radiation. The temperature sensors were fixed along the axis of the cylinders in the same way as in the original detector cylinder. The source–surface distance (distance between the surface of the calorimeter water phantom and the ^{60}Co-γ-source) was chosen such that the dose rate amounted to 0.66 Gy/min at the reference depth (5 cm), decreasing almost linearly over the dimensions of the detector vessel as a function of the depth in the water phantom. The investigations were performed for a water temperature of 4°C [7].

The measurements concerning the electrical heating of the thermistors were performed in the same setup. The thermistors used have a diameter of 0.25 mm and, at the manufacturers, have been embedded in the tip of a glass rod 0.5 mm in diameter and 8 mm in length. In the experiment the electrical power was instantaneously varied in the μW range by changing the voltage supply to the thermistors. The corresponding change in the thermistor temperature was determined as a function of time.

3. Results and discussion

3.1. Irradiation of the cylinder walls

The experimental results and the results of the numerical computations are presented in Fig. 2 for a PMMA cylinder 30 mm in diameter and with a wall
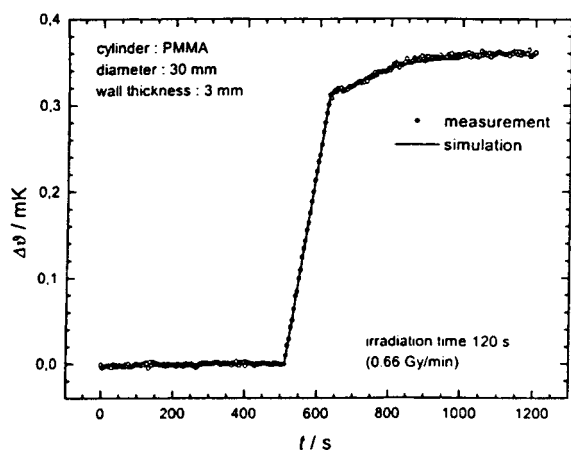
Fig. 2. Experimental results and results obtained by numerical computations for a PMMA cylinder. The temperature variation is plotted as a function of time around an irradiation period with ^{60}Co-γ-radiation (dose rate: 0.66 Gy/min, irradiation time: 120 s). For the sake of clarity, only a fraction of the experimental data is presented.

Fig. 3. Deviation of the radiation-induced temperature rise, with heat conduction influences allowed for, from the temperature rise, with such influences disregarded (excess temperature), in relation to the latter as a function of the time after beginning of irradiation, computed for PMMA cylinders (dose rate: 0.66 Gy/min, irradiation time: 120 s).

thickness of 3 mm. The temperature variation has been plotted as a function of time around an irradiation period with ^{60}Co-γ-radiation (dose rate: 0.66 Gy/min, irradiation time: 120 s). For the period of up to about 120 s after the end of the irradiation, which is of significance in practice for the extrapolation of the post-period of the caloric measurement, agreement is satisfactory. Towards longer periods of time, heat conduction influences due to the irradiation of the more massive cylinder end faces make themselves felt, which have not been taken into account in the computations.

Fig. 3 shows the deviation of the radiation-induced temperature rise with heat conduction influences allowed for, from the temperature rise, with such influences disregarded (excess temperature), for PMMA cylinders 30 mm in diameter and with wall thicknesses of 2 and 3 mm, under identical irradiation conditions. The numerically computed values have been plotted in percent, as a function of the time after beginning of exposure. The effect, which is independent of dose rate, rapidly decreases with decreasing wall thickness, and it can be further reduced when the irradiation time is shortened.

To keep low both, the heat transport influences discussed here and the radiation field perturbation due to the cylinder wall, the wall thickness of the
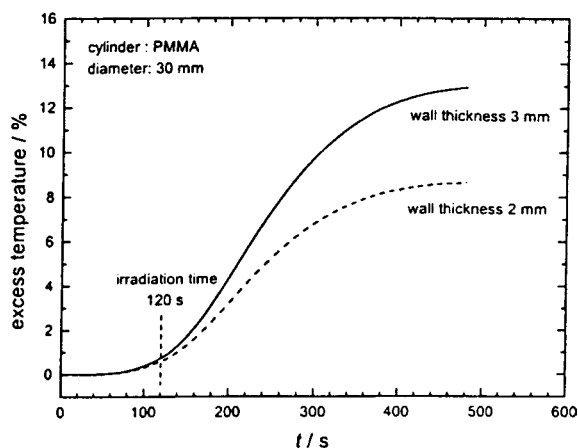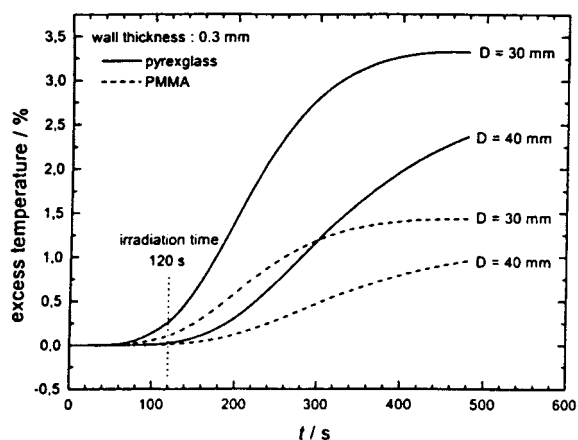

Fig. 4. Deviation of the radiation-induced temperature rise, with heat conduction influences allowed for, from the temperature rise, with such influences disregarded (excess temperature), in relation to the latter as a function of the time after beginning of irradiation, computed for cylinders of different diameters made of glass and PMMA (dose rate: 0.66 Gy/min, irradiation time: 120 s).

detector glass cylinders of the water absorbed dose calorimeter used in practice is smaller than 0.3 mm in measurements where highest accuracy is required. For the irradiation conditions of Figs. 2 and 3, the excess temperature is in this way reduced by about one order of magnitude (Fig. 4). For an irradiation time of 60 s, a

correction of less than 0.3% results for a glass cylinder of 40 mm in diameter and with a wall thickness of 0.3 mm. It is reduced to about 0.1% if only a period of 60 s during the post-period is used for extrapolation. For cylinders with larger diameter even lower corrections apply.

Depending on the measurement tasks, different dimensions can be selected for the detector vessel of the calorimeter, resulting in different heat conduction corrections. For use as a primary standard measuring device in a ^{60}Co-γ-radiation field, for instance, the correction can be kept below 0.1%. Large vessel diameters lead, however, to considerable temperature equilibration times after a set of irradiations (if the water inside the vessel is not stirred before the irradiations in order to ensure a homogeneous temperature distribution), and thin walls make the vessels fragile. Whereas this does not really constitute a problem for a primary standard, the application of the calorimeter as a transfer standard requires more robust vessels with smaller volumes. The present investigations show that the excess heat correction of such vessels may amount to a few 0.1% which can, however, usually be corrected with a relative standard uncertainty of the order of 0.1%.

3.2. Irradiation of the temperature probes

The excess temperature created directly in the thermistors and in the glass pipettes by radiation absorption was experimentally investigated in a previous publication [9]. This effect depends on the dose rate and on the thermal properties and the radiation interaction parameters for the thermistor and the glass. It was shown that the excess temperature at the end of the irradiation amounts to a few μK, and that it drops down to almost zero within about 10 s so that the influence on the extrapolation of the calorimeter post-period may be kept negligibly small.

In order to separate the effects of radiation interaction and to check the thermal parameters, the electrical heating of the thermistors has, in addition, been studied experimentally, enabling additional benchmarks of the model calculations.

The corresponding finite element model of the temperature probe was used to calculate the variation of the thermistor temperature as a function of time for an increase (decrease) of the electrical power. The
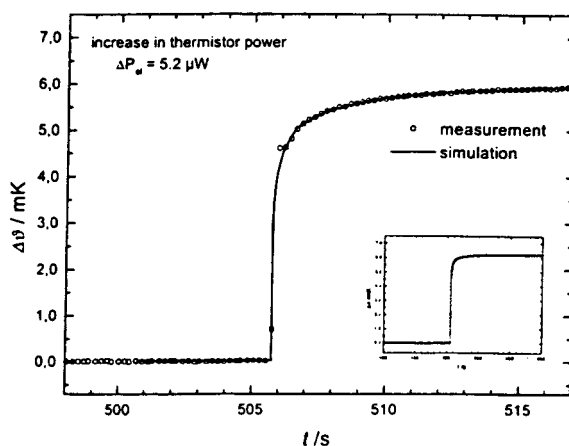

Fig. 5. Comparison between calculated and experimental values for the temperature change of the thermistors as a function of time after an instantaneous increase of the thermistors' electrical power.

calculations indicate that the transient course of the resulting heating (cooling) curve strongly depends on the specific heat capacity chosen for the thermistor material and that the stationary part is mainly determined by the corresponding thermal conductivity. The thermal properties used for the simulations are in accordance with the data given by the manufacturers. Fig. 5 shows the results of the finite element calculations and the data of the caloric measurements for a change in electrical power of 5.2 μW; the calculated equilibrium temperature was normalized to the experimental value. When the same finite element model is used to simulate the excess temperature caused directly in the thermistors and in the glass pipettes by radiation, the results agree with the experimental results [9].

4. Conclusions

The present investigations show that optimization of the detector vessels can keep the correction of the heat transport effects caused by the material-dependent temperature rise in the detector walls and in the temperature probes embedded in water below 0.1% for irradiation conditions similar to the reference conditions at ^{60}Co-γ-radiation. The agreement between the results of the model calculations and of the corresponding benchmark experiments shows,

however, that the correction of these effects is accurate enough to allow essentially more robust vessels with smaller dimensions to be used for applications allowing slightly increased uncertainties. The energy deposition pattern may then be calculated by Monte Carlo simulations which, as heat source distributions, are input in the finite element calculations.

References

[1] S.R. Domen, J. Res. Nat. Bur. Stand. 87(3) (1982) 211–235.

[2] C.K. Ross, N.V. Klassen, Phys. Med. Biol. 41 (1996) 1–29.

[3] N.V. Klassen, C.K. Ross, Radiat. Phys. Chem. 38(1) (1991) 95.

[4] A. Krauss, M. Roos, Thermochim. Acta 229 (1993) 125–132.

[5] M. Roos, in: C.K. Ross, N.V. Klassen (Eds.), NRC Workshop on Water Calorimetry, NRC Publication 29637, Ottawa, 1988, p. 9.

[6] M. Roos, Thermochim. Acta 119 (1987) 81–93.

[7] S.R. Domen, A. Krauss, Thermochim. Acta 187 (1991) 225–233.

[8] A. Krauss, M. Roos, NPL Calorimetry Workshop, Teddington, 1994.

[9] A. Krauss, M. Roos, Thermochim. Acta 310 (1998) 53–60.

[10] S.R. Domen, J.Res. Natl. Stand. Technol. 99 (1994) 121.

[11] H. Palmans, J. Seuntjens, NPL Calorimetry Workshop, Teddington, 1994.

[12] J. Seuntjens, C.K. Ross, N.V. Klassen, K.R. Shortt, A status report on the NRC sealed water calorimeter, Technical Report PIRS-584, NRC Canada, Ottawa, 1997.

[13] H. Palmans, J. Seuntjens, Phys. Med. Biol. 44 (1999) 627–646.